



Label-free quantitative proteomics in serum reveals candidate biomarkers associated with low bone mineral density in Mexican postmenopausal women

Diana I. Aparicio-Bautista · Adriana Becerra-Cervera · Berenice Rivera-Paredes · Israel Aguilar-Ordoñez · Emmanuel Ríos-Castro · Juan P. Reyes-Grajeda · Jorge Salmerón · Alberto Hidalgo-Bravo · Rafael Velázquez-Cruz

Received: 4 July 2023 / Accepted: 7 October 2023 / Published online: 24 October 2023
© The Author(s), under exclusive licence to American Aging Association 2023

Abstract Postmenopausal osteoporosis is a public health problem leading to an increased risk of fractures, negatively impacting women's health. The absence of sensitive and specific biomarkers for early detection of osteoporosis represents a substantial challenge for improving patient management. Herein, we aimed to identify potential candidate proteins associated with low bone mineral density (BMD) in

postmenopausal women from the Mexican population. Serum samples from postmenopausal women (40 with normal BMD, 40 with osteopenia (OS), and 20 with osteoporosis (OP)) were analyzed by label-free LC-MS/MS quantitative proteomics. Proteome profiling revealed significant differences between the OS and OP groups compared to individuals with normal BMD. A quantitative comparison of proteins between groups indicated 454 differentially expressed proteins (DEPs). Compared to normal BMD, 14 and 214 DEPs were found in OS and OP groups, respectively, while 226 DEPs were identified between OS and OP groups. The protein-protein interaction and

Diana I. Aparicio-Bautista and Adriana Becerra-Cervera contributed equally to this work and share first authorship.

Supplementary Information The online version contains supplementary material available at <https://doi.org/10.1007/s11357-023-00977-1>.

D. I. Aparicio-Bautista · J. P. Reyes-Grajeda
Laboratorio de Estructura de Proteínas, Instituto Nacional de Medicina Genómica (INMEGEN), 14610 Ciudad de Mexico, Mexico

A. Becerra-Cervera · R. Velázquez-Cruz (✉)
Laboratorio de Genómica del Metabolismo Óseo, Instituto Nacional de Medicina Genómica (INMEGEN), 14610 Ciudad de Mexico, Mexico
e-mail: rvelazquez@inmegen.gob.mx

A. Becerra-Cervera
Consejo Nacional de Humanidades, Ciencias y Tecnologías (CONAHCYT), 03940 Ciudad de Mexico, Mexico

B. Rivera-Paredes · J. Salmerón
Centro de Investigación en Políticas, Población y Salud, Facultad de Medicina, Universidad Nacional Autónoma de México, 04510 Ciudad de México, Mexico

I. Aguilar-Ordoñez
Departamento de Supercómputo, Instituto Nacional de Medicina Genómica (INMEGEN), 14610 Ciudad de Mexico, Mexico

E. Ríos-Castro
Unidad de Genómica, Proteómica y Metabolómica (UGPM), LaNSE, Cinvestav-IPN, 07360 Ciudad de Mexico, Mexico

A. Hidalgo-Bravo (✉)
Departamento de Medicina Genómica, Instituto Nacional de Rehabilitación, 14389 Ciudad de México, Mexico
e-mail: dr_genetica@yahoo.com

enrichment analysis of DEPs were closely linked to the bone mineral content, skeletal morphology, and immune response activation. Based on their role in bone metabolism, a panel of 12 candidate biomarkers was selected, of which 1 DEP (RYR1) was found upregulated in the OS and OP groups, 8 DEPs (APOA1, SHBG, FETB, MASP1, PTK2B, KNG1, GSN, and B2M) were upregulated in OP and 3 DEPs (APOA2, RYR3, and HBD) were downregulated in OS or OP. The proteomic analysis described here may help discover new and potentially non-invasive biomarkers for the early diagnosis of osteoporosis in postmenopausal women.

Keywords Serum · Proteomics · Bone mineral density · Postmenopausal women · Biomarkers · Mexican population

Introduction

Osteoporosis (OP) is a systemic skeletal disease characterized by low bone mineral density (BMD), with a consequent increased risk of suffering fragility fractures [1]. Postmenopausal osteoporosis is a major public health problem affecting women's health negatively. OP is associated with estrogen deficiency, resulting in an imbalance of bone turnover and inducing the rapid loss of bone [2]. According to the World Health Organization (WHO), OP-related fractures occur in 20% of men and in 33% of women during their lifetime after the age of 50 years [3, 4], which implies a direct economic burden for health systems worldwide. In México, by the year 2010, the direct cost caused by more than 75,000 fragility fractures was estimated at 256.2 million dollars, and it is projected to increase to 350,000 cases in 2030 [5, 6]. These facts emphasize the importance of developing novel and effective strategies for early diagnosis of OP and fracture risk assessment.

Clinically, dual-energy X-ray absorptiometry (DXA) is the gold standard for BMD evaluation and OP diagnosis [7]. However, the use of BMD as the exclusive resource for BMD assessment is problematic for many reasons [8], such as the low sensitivity for fracture prediction, the need for dedicated facilities, elevated costs, large dimensions of equipment, and trained personnel. All these factors could be inaccessible for vulnerable groups,

particularly in less-developed countries. An alternative for the early diagnosis of OP might be the measurement of plasma or serum proteins, which is a minimally invasive procedure, and current evidence supports the potential clinical value of this method [9]. Besides, although many studies have reported serum biochemical parameters as predictors of osteoporosis (e.g., calcium, creatinine, alkaline phosphatase), they do not provide a definable pathway linking bone metabolism because they could be influenced by several exogenous factors, such as circadian rhythm, diet, physical activity, and seasonal variation [10, 11].

Recent advances in proteomics technologies have prompted the search for early biomarkers of the condition of bone and follow-up of the treatment efficacy [12]. Therefore, quantitative proteomics approaches using common fluids could be helpful for both the early detection of OP and the evaluation of bone status [13]. Numerous studies have proposed serum biomarkers associated with high bone turnover and BMD in postmenopausal women [11]. Although identifying the proteins and metabolic pathways involved in regulating bone metabolism in different populations has increased, the precise knowledge of the biological mechanisms underlying BMD is incomplete [14–17]. Conventional protein-based markers have some limitations regarding pre-analytical, analytical, and post-analytical factors, including a lack of specificity and sensitivity, which limits their clinical applicability [18]. Previously, our group conducted a proteomic analysis using two-dimensional differential gel electrophoresis (2D-DIGE) in 446 postmenopausal women. We found three relevant proteins associated with BMD: ceruloplasmin, gelsolin, and vitamin D-binding protein (VDBP). Our results directly correlated VDBP levels with BMD values [19].

This study aimed to identify novel candidate proteins as biomarkers related to low BMD in postmenopausal Mexican women, using quantitative liquid chromatography coupled to mass spectrometric (LC–MS), and computational resources. These novel protein biomarkers could be clinically helpful for early diagnosis of OP and open a window of opportunity, providing scientific knowledge for further research on bone health.

Materials and methods

Study population

Serum samples from 446 unrelated postmenopausal women were collected. Subjects recruited in this study were derived from a prospective cohort study, “The Health Workers Cohort Study (HWCS),” from the Mexican Social Security Institute (IMSS) [20]. The HWCS is a long-term study of workers from the IMSS in Cuernavaca, Morelos, focusing on lifestyle and the development of chronic diseases. All women included in this study had Mexican-Mestizo origin. Samples were collected in the third assessment from 2016 to 2019. The detailed characteristics of postmenopausal women were previously reported [19].

A subgroup of 100 postmenopausal women (40 with normal BMD, 40 with osteopenia (OS), and 20 with osteoporosis (OP)) was selected for the

proteomic analysis (Table 1). Women were selected based on the following inclusion criteria: ≥ 45 years old, menopause confirmed (12 consecutive months without menstruation), and available BMD measures. Women with diabetes mellitus, chronic liver diseases, rheumatoid arthritis, collagen diseases, endocrine disorders affecting bone metabolism (e.g., parathyroid, gonadal, adrenal, and thyroid diseases), and those taking corticosteroids, anticonvulsants, bisphosphonates, or hormone replacement were excluded.

The protocol was approved by the ethics committees from the Mexican Social Security Institute (No. 12CEI 09 006 14), and the National Institute of Genomic Medicine (266–17/2016/I). All procedures were conducted in accordance with the Declaration of Helsinki (13/LO/0078). All participants provided written informed consent. Demographic and clinical data of the study population are reported in Table 1.

Table 1 Demographic and clinical characteristics of the study population

| | N (<i>n</i> =40) | OS (<i>n</i> =40) | OP (<i>n</i> =20) | OS vs. N <i>p</i> -value | OP vs. N <i>p</i> -value | OP vs. OS <i>p</i> -value |
|---------------------------------------|----------------------------|----------------------------|----------------------------|-----------------------------|-----------------------------|------------------------------|
| Age (years) | 56 (49.5–61.5) | 66 (59–71) | 70.5 (63.5–76) | 0.0002 | <0.001 | 0.033 |
| BMI (kg/m ²) | 25.9 (24.1–27.3) | 25.0 (23.1–26.8) | 23.3 (20.8–26) | 0.0871 | 0.0041 | 0.0625 |
| Total hip BMD (g/cm ²) | 0.969 (0.943–0.991) | 0.799 (0.783–0.822) | 0.66 (0.641–0.676) | <0.001 | <0.001 | 0.0001 |
| Lumbar spine BMD (g/cm ²) | 1.061 (1.001–1.134) | 0.939 (0.855–1.006) | 0.793 (0.696–0.870) | 0.0001 | <0.001 | 0.0005 |
| Femoral neck BMD (g/cm ²) | 0.925 (0.890–0.962) | 0.762 (0.745–0.784) | 0.620 (0.586–0.643) | <0.001 | <0.001 | 0.0001 |
| T-score, total hip | −0.311 (−0.510, −0.131) | −1.660 (−1.786, −1.471) | −2.73 (−2.913, −2.634) | <0.001 | <0.001 | 0.0001 |
| T-score, lumbar spine | −1.264 (−1.688, −0.561) | −2.175 (−2.716, −1.569) | −3.304 (−3.857, −2.641) | <0.001 | <0.001 | 0.0006 |
| T-score, femoral neck | −0.814 (−1.064, −0.545) | −1.964 (−2.109, −1.821) | −3.004 (−3.234, −2.792) | <0.001 | <0.001 | 0.0002 |
| Body fat proportion | 43.6 (39.4–46.2) | 43.2 (39.5–46.6) | 39.4 (34.0–42.8) | 0.332 | 0.007 | 0.0022 |
| Waist circumference (cm) | 87 (83–92) | 85 (81–91) | 85 (76–91) | 0.136 | 0.0322 | 0.169 |
| Vitamin D intake (UI/day) | 108.0 (46.5–201.5) | 103.5 (61.2–177.4) | 67.7 (27.0–154.2) | 0.466 | 0.109 | 0.122 |
| Calcium intake (UI/day) | 594.7 (466.3–904.2) | 548.3 (391.7–813.9) | 577.4 (335.8–1093.7) | 0.205 | 0.281 | 0.463 |
| Vitamin D supplementation (%) | 12.5 | 12.5 | 15 | 1 | 0.788 | 0.788 |
| Calcium supplementation (%) | 17.5 | 27.5 | 40 | 0.284 | 0.057 | 0.326 |

Data are expressed as the median (inter-quartile range) or percentage. *N* normal, *OS* osteopenia, *OP* osteoporosis, *BMI* body index mass, *BMD* bone mineral density

Bone mineral density (BMD) and osteoporosis diagnosis

Hip BMD (g/cm^2) was determined using a Lunar DPX NT dual-energy X-ray absorptiometry (DXA) instrument (Lunar Radiation Corp., Madison, WI, USA). Subjects were categorized into three groups according to their hip T-score, using the criteria defined by the WHO to determine low BMD [21, 22]. The normal group (N) included women with T-scores above -1.0 , the osteopenic group (OS) included women with T-scores from -1.0 to -2.5 , and the osteoporotic group (OP) women with T-scores below -2.5 .

Serum sample preparation for LC–MS analysis

Blood samples were collected from all patients by the same operator with at least 2 h of fasting and left to clot for 30 min. After centrifugation at $2643 \times g$ for 15 min, serum was extracted, frozen, and stored at $-80\text{ }^\circ\text{C}$ until use. Ten serum samples from each group were pooled to make four pools for N and OS, while five samples shaped the OP pools to make four pools because of the limited number of samples with similar clinical characteristics.

Albumin, IgG, antitrypsin, IgA, transferrin, haptoglobin, fibrinogen, alpha2-macroglobulin, alpha1-acid glycoprotein, IgM, apolipoprotein AI, apolipoprotein AII, complement C3, and transthyretin were depleted from the protein pools using the Multiple Affinity Removal Column Human 14 (Agilent, Santa Clara, CA, USA) on an AKTA Pure chromatography system (Cytiva, Marlborough, MA, USA).

Depleted pools were quantified using a 2D Quant Kit (GE Healthcare, Chicago, IL, USA), following the manufacturer's instructions. Afterwards, $50\text{ }\mu\text{g}$ of protein was enzymatically digested using PreOmics iST Sample Preparation Kit® (PreOmics GmbH, Munich, Germany) according to the protocol established by the manufacturer. The resulting peptides were cleaned, eluted, and evaporated to dryness in a SpeedVac Savant (Thermo Fisher Scientific, Waltham, MS, USA). Finally, peptides were resuspended and stored at $-80\text{ }^\circ\text{C}$ until LC–MS analysis [23].

Label-free quantitative proteomics

The quantitative LC–MS analytical method was applied as described in Ríos-Castro et al. [24] with some modifications. Briefly, tryptic peptides were injected into the mass spectrometer Synapt G2-Si (Waters, Milford, MA) in Multiplexed MS/MS (MS^E) mode to calculate the area under curve (AUC) of the total ion chromatogram (TIC), with the aim of normalizing the amount of tryptic peptides in each injection during the label free analysis. Afterwards, peptides were loaded and separated on an HSS T3 C18 column (Waters, Milford, MA). The spectra data were acquired by the mass spectrometer using nano electrospray ionization (nanoESI) and ion mobility separation (IM-MS) using a data-independent acquisition (DIA) approach through High-Definition Multiplexed MS/MS (HDMS^E) mode. For the ionization source, parameters were set with the following values: 2.75 kV in the capillary emitter, 30 V in the sampling cone, 30 V in the source offset, $70\text{ }^\circ\text{C}$ for the source temperature, 0.5 bar for the nanoflow gas and $150\text{ L}\cdot\text{h}^{-1}$ for the purge gas flow. Two chromatograms were acquired (low- and high-energy chromatograms) in the positive mode range of m/z 50–2000 with a scan time of 500 ms. No collision energy was applied to obtain the low-energy chromatograms, while for the high-energy chromatograms, the precursor ions were fragmented in the transfer cell using a collision energy ramp from 19 to 55 eV.

Data search

The MS and MS/MS measurements were analyzed and relatively quantified by Progenesis QI for Proteomics software v3.0 [25] (Waters, Milford, MA) using a target decoy strategy against a *Homo sapiens* *.fasta database (obtained from UniProt, UP000005640, 79052 protein sequences), which was concatenated with the same *.fasta file in the reverse sense [26]. Parameters used for the protein identification were trypsin as cutting enzyme and one missed cleavage allowed; carbamidomethyl (C) as a fixed modification and oxidation (M), amidation (C-terminal), deamidation (Q, N), and phosphorylation (S, T, Y) as variable modifications; default peptide and fragment tolerance (maximum normal distribution of 10 and 20 ppm respectively) and false discovery rate $\leq 4\%$; all false positive identifications

(reversed proteins) were discarded for subsequent analysis. Synapt G2-Si was calibrated with [Glu1]-fibrinopeptide fragments through the precursor ion $[M + 2H]^{2+} = 785.84261$ fragmentation of 32 eV with a result of less than 1 ppm across all MS/MS measurements. The quality control analysis exhibited an adequate adjustment in calibration, ionization source operability, enzymatic effectiveness, and database searching (Supplementary Fig. 1).

Bioinformatic and statistical analysis

Proteomic data were filtered following the criteria of ≥ 2 peptides and at least one unique peptide. To identify any clustering or separation of the compared datasets, the partial least squares discriminant analysis (PLS-DA) model and the unsupervised principal component analysis (PCA) of the protein abundance scale were performed. PLS-DA and PCA scores were extracted using package `rolps`. For the three-dimensional representation of proteome data between groups, the `scatterplot3d` package was used. Student's *t*-test was performed for each pairwise comparison (OP vs. N, OS vs. N, and OP vs. OS) to identify the differentially expressed proteins (DEPs). DEPs were selected based on two criteria: fold change > 1.5 or < 1.5 and a false discovery rate (FDR) adjusted p -value < 0.05 . Associations of hip BMD with proteins were assessed by linear regression using the `lm` function adjusting for age. A second model was examined with further adjustments for BMI, calcium intake, and vitamin D intake. Furthermore, receiver operating characteristic (ROC) curves were constructed using the protein abundance adjusted for age. The area under the ROC curve (AUC), the 95% confidence interval (CI), sensitivity, and specificity analyses were performed using `pROC` package. Spearman correlation was performed using the protein abundance adjusted for age and clinical information. Statistical significance was defined as FDR-corrected p -value < 0.05 .

The online tool Searching The Retrieval of Interacting Genes/Proteins (STRING, <https://string-db.org>) was used for construction of protein–protein interaction (PPI) network. The PPI network was constructed by setting medium confidence at 0.400. All DEPs by mass spectrometry were used for building the PPI network.

The Gene Ontology (GO) enrichment of differentially expressed proteins were performed by package `clusterProfiler` in R [27]. GO results were categorized into three modules, including biological process (BP), molecular functions (MF), and cellular compartment localization (CC). The results with an FDR-corrected p -value < 0.05 were considered significant.

PCA and PLS-DA analysis of proteome data, volcano plots of DEPs, functional enrichment, and statistical analyses were conducted using R 4.1.0. All the workflow and the specific criteria of the analysis are available on GitHub (https://github.com/Iaguilaror/low_BMD_in_PMWMX).

Results

Study population

A total of 100 postmenopausal women from the HWCS were included in this study. Participants were divided according to their BMD value into three groups: normal BMD ($n=40$), osteopenia ($n=40$), and osteoporosis ($n=20$). The median age was significantly higher in the OS (66 years) and OP (70.5 years) groups versus the N group (56 years) ($p < 0.001$). In addition, a significant difference in median age was also observed when comparing the OS group versus the OP group ($p < 0.05$). BMD in total hip, lumbar spine, and femoral neck were significantly lower in OS and OP groups compared to the normal group ($p < 0.001$). The OP group presented lower BMI and body fat proportion than the normal group ($p < 0.005$) (Table 1). Triglycerides were higher in OS and OP ($p < 0.05$) compared to the normal group, while HDL was lower only in the OS group compared to the normal group ($p < 0.05$). No statistically significant differences between groups regarding cholesterol, glucose, and physical activity were observed (Supplementary Table 1).

Proteomic profiling and protein differential expression analysis

Eight hundred seventy-four proteins were identified in the serum samples of the N, OS, and OP groups through label-free mass spectrometry-based protein quantification (Supplementary Table 2). As shown in Fig. 1A, the Venn diagram shows 723 (83%)

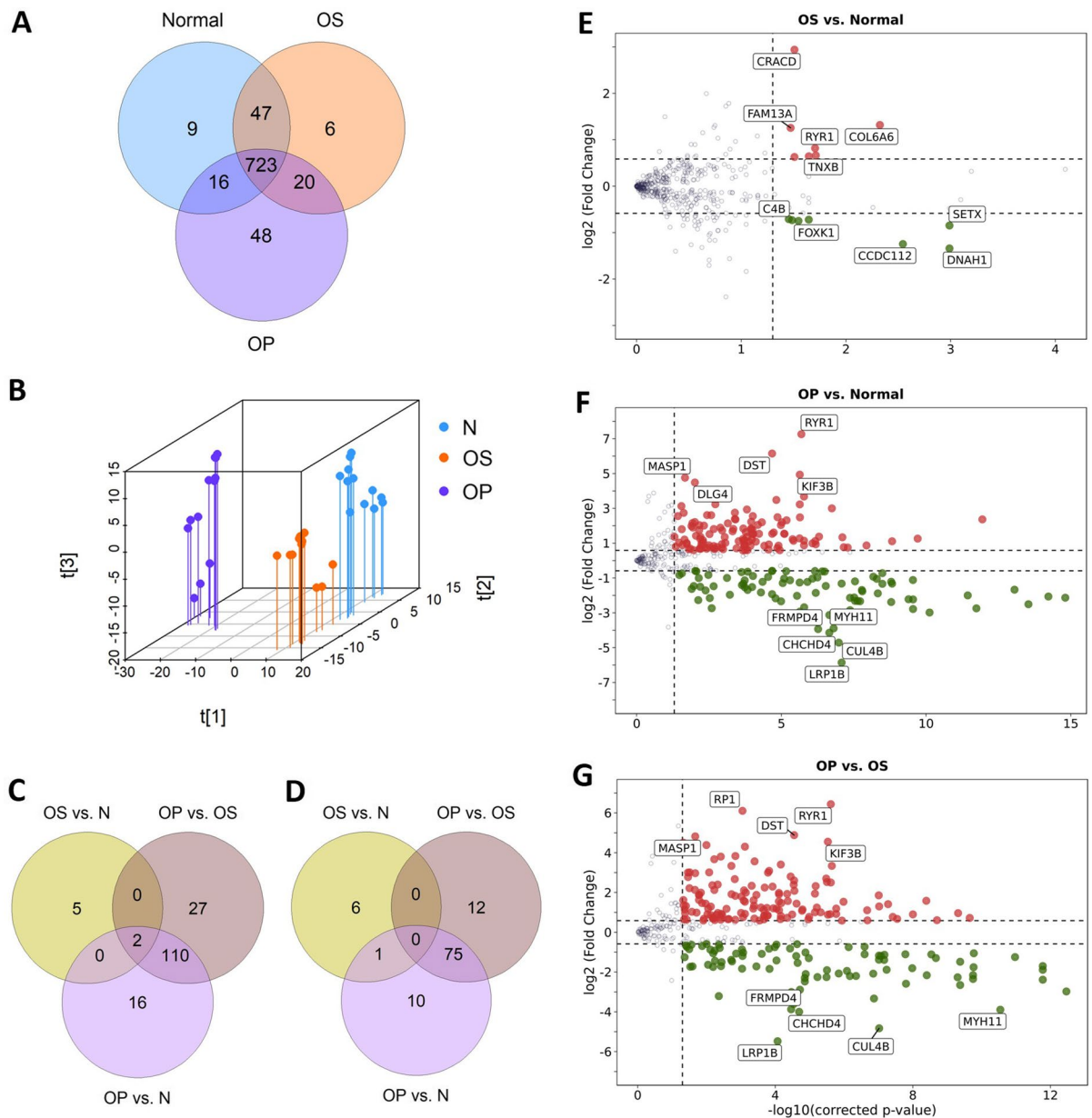


Fig. 1 Profile of proteins identified in the serum of the study groups and their differential expression between groups. **A** Total number of proteins identified and those shared among the Normal (N), osteopenic (OS), and osteoporotic (OP) postmenopausal women. **B** Three-dimensional of partial least squares discriminant analysis (PLS-DA) of global proteome data. Blue dots represent an individual injection of normal group samples, orange dots the OS group, and the purple dots the OP group; each sample pool per group ($n=4$) was injected by triplicate. **C** Number of shared and unique DEPs upregulated and

D downregulated between groups. **E–G** Volcano plots displaying proteins with significantly different abundance between OS vs. N, OP vs. N, and OP vs. OS, respectively. The x-axis and y-axis on the volcano plot represented the \log_2 -fold change between the two comparison groups and the \log_{10} p -value, respectively. Red dots represent the upregulated proteins, and green dots represent the downregulated proteins. Each volcano plot shows the protein ID with the highest or lowest changes in abundance per condition

overlapping proteins among the three study groups. Furthermore, 47 proteins overlapped between the OS and Normal groups, 16 between the OP and Normal groups, and 20 between the OS and OP groups. Additionally, 9 proteins were exclusively expressed in the Normal group, 6 in the OS group and 48 in the OP group. The proteomics pattern associated with the three study groups was examined using the partial least squares discriminant analysis (PLS-DA) and unsupervised principal component analysis (PCA). As shown in Fig. 1B, group separation and sample clustering between the Normal, OS, and OP groups ($R^2 X=0.604$, $R^2 Y=0.991$, $Q^2=0.94$) were observed, indicating proteomics differences between these three groups. In particular, the data evidenced a clear separation between OS and OP (low BMD), especially when discriminating between OP and Normal groups (Supplementary Fig. 2), whereas the clustering of the OS and normal groups revealed less-than-ideal effects on the separation between proteomic profiles (Fig. 1B). PLS-DA and PCA plots between groups are shown in Supplementary Fig. 2.

The Venn diagrams (Fig. 1C–D) illustrate the number of upregulated and downregulated DEPs between comparisons. Five and sixteen proteins were upregulated as unique in OS or OP vs. N, respectively. Twenty-seven were uniquely upregulated proteins between OP vs. OS. Six downregulated proteins were unique in OS vs. N and ten in OP vs. N. Twelve DEPs were downregulated between OP vs. OS. Most upregulated and downregulated DEPs overlapped in OP or OS vs. N. The total number of DEPs between comparisons is Supplementary Fig. 3. Volcano plots show the statistical distributions of differentially expressed proteins by condition, each diagram showing the protein symbol of the five most over- and down-expressed proteins (Fig. 1E–G). All specific data about over- and down-expressed proteins between the groups analyzed are in Supplementary Table 3.

Protein–protein interaction analysis between DEPs

To understand the relationship between the DEPs identified in OS and OP groups, the STRING database was employed to construct a PPI network. Figure 2A shows the down-expressed proteins network in OS and OP; the biological network was composed by 92 nodes and 160 edges with a PPI enrichment of p value $< 1.0 \times 10^{-16}$. We found 22 proteins

associated to skeletal system (BTO:0001486) such as VTN, APOB, TTR, C3, APCS, VWF, CP, PREX2, FYCO1, A2M, SERPINA5, CDH5, FILIP1L, APOA2, RYR3, PROS1, CFI, CUL4B, XIRP2, C4A, C4B, and C1R (red nodes). According to KEGG pathway enrichment analysis, some proteins are associated with complement and coagulation cascades (F9, C8G, VTN, C3, VWF, C9, C7, A2M, SERPINA5, C8B, F10, PROS1, CFI, C4A, C4B, and C1R). On the other hand, the Fig. 2B shows the over-expressed proteins network in OS and OP, composed by 129 nodes and 273 edges with a high interaction between them (p value $< 1.0 \times 10^{-16}$). This analysis revealed 42 proteins participating in abnormal skeletal morphology (HP:0011842) (pink nodes) and 40 proteins in abnormality of the skeletal system (HP:0000924) (blue nodes). In this biological network, we can find proteins involved in osteoporosis (HP000939), reduced bone mineral density (HP0004349), bone fracture related to measurement (EFO:0004516) and bone measurement (EFO:0004512), such as POLG, WRN, HSPG2, F2 FGFR2, SYNE1, DLG4, DNAH11, TNXB, BNC2, ARIDA1, DST, RYR1, FBXO11, CLIP1, SYNE1, and CNOT1. All specific data about the PPI network including GO process, GO function and GO component are in Supplementary Table 4.

Functional enrichment analysis

Gene Ontology analysis was performed to identify the functional categories of DEPs. As shown in Fig. 3A, most DEPs in the OS and OP related to the N group were enriched in blood microparticle,

collagen-containing extracellular matrix, humoral immune response, endoplasmic reticulum lumen, wound healing, and others. Particularly, biological processes were significantly enriched in humoral immune response, wound healing, complement activation, regulation of body fluid levels, and micro-tubule-based movement (Fig. 3B). While most identified proteins were enriched in enzyme inhibitor activity, phospholipid binding, peptidase regulator activity, endopeptidase inhibitor activity, and peptidase inhibitor activity (Fig. 3C), proteins were enriched in blood microparticle, followed by collagen-containing extracellular matrix and endoplasmic reticulum lumen (Fig. 3D).

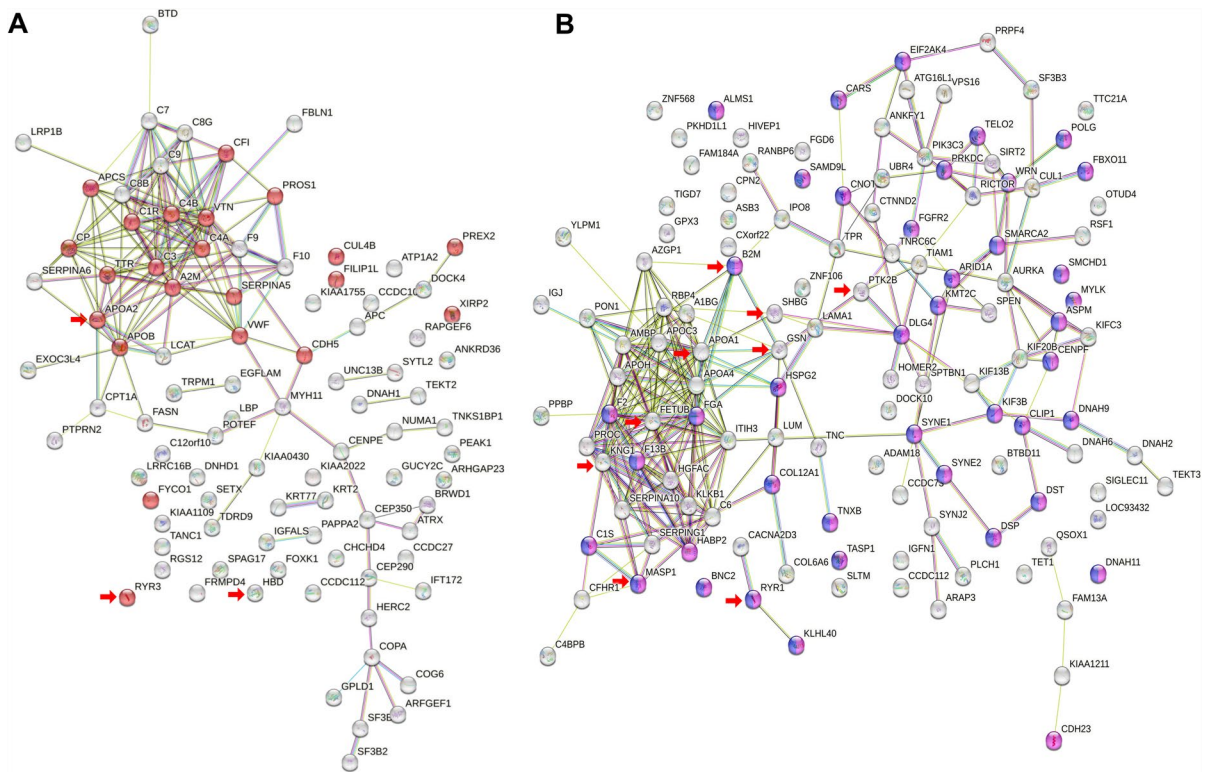


Fig. 2 PPI networks of DEPs associated with OS and OP vs normal group visualized by STRING. The PPI network was constructed by setting the medium confidence at 0.400. Network nodes represent proteins, and edges represent protein–protein associations. **A** Downregulated proteins in OS and OP respect to the N group, the red nodes indicate those proteins

associated to Skeletal system. **B** Upregulated proteins in OS and OP respect to the N group, the blue nodes show those proteins linked to the abnormality of the skeletal system, and the pink nodes show those proteins related in abnormal skeletal morphology. Arrows indicate the 12 proteins proposed as possible biomarkers in low BMD

Proteins selected as candidate biomarkers in the serum of patients with low BMD

The proteins were selected as potential markers according to two criteria: (1) a significant differential expression in OS or OP, or both, with respect to the normal group; (2) proteins involved in bone metabolism and processing, osteopenia, osteoporosis, and calcium pathway according to the PPI analysis and literature review. Based on these criteria, 12 DEPs were selected as potential non-invasive serum protein biomarkers for low BMD (Table 2). After FDR-corrected p -value, one (RYR1) was found upregulated in the OS and OP groups, eight (APOA1, SHBG, FETB, MASP1, PTK2B, KNG1, GSN, and B2M) were upregulated only in the OP group. At the same time, three proteins (APOA2, RYR3, and HBD) were downregulated in OS or OP groups. Figure 4 depicts

the comparison of the serum levels of these 12 proteins between the three study groups.

Verifying the association of candidate biomarkers with changes in bone mineral density was examined using linear regression. There were nine proteins (APOA1, FETB, B2M, PTK2B, RYR1, KNG1, SHBG, MASP1 and GSN) were negatively associated and three proteins (APOA2, HBD, and RYR3) were positively associated with hip BMD in the basic model (FDR p -value < 0.05) and adjustments for age, BMI, calcium intake, and vitamin D intake (FDR p -value < 0.05) (Supplementary Table 5).

ROC curves were generated for further examination of the potential clinical utility of the candidate biomarkers for osteoporosis and osteopenia diagnosis. Six proteins allowed the recognition of OP individuals when compared to the N group (FDR p -value < 0.05), harboring RYR1, KNG1, and

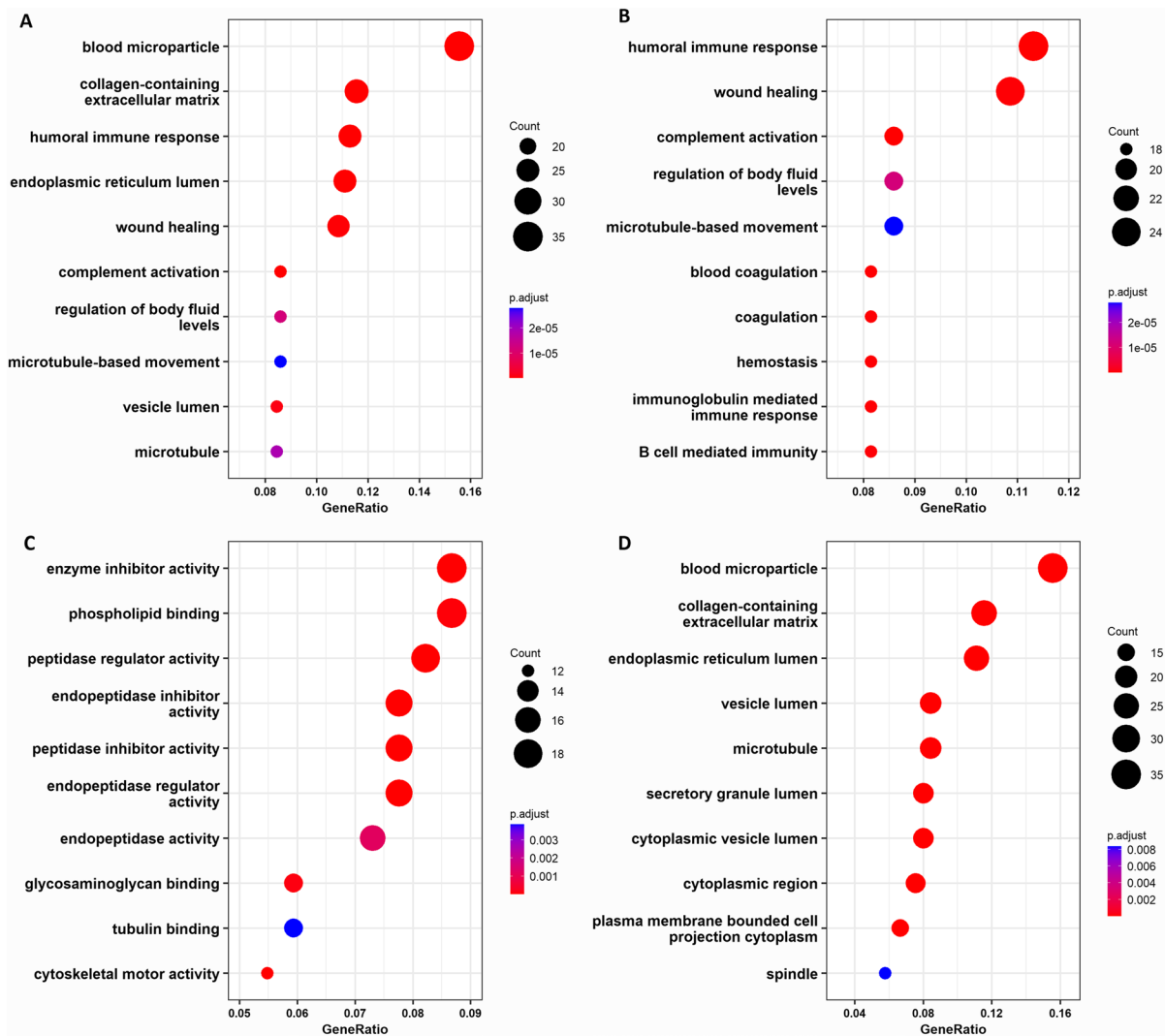


Fig. 3 GO functional annotation of the DEPs. **A** General GO enrichment analysis of DEPs between OS and OP vs. N. The GO annotations are classified into three different categories, including **B** biological process, **C** molecular functions, and **D**

cellular components. The size of the dots indicates the number of proteins related to each function, and the gradient color scale indicates the *p*-value

GSN the highest diagnostic capacity (AUC = 100%, 100%, and 99.3%, respectively) (Supplementary Fig. 4 A–C). In addition, four proteins (GSN, KNG1, FETB, and APOA2) allowed the specific diagnosis of osteopenia, providing AUC values above 75% when compared with the normal group (FDR *p*-value < 0.05) (Supplementary Fig. 4 D–F). Furthermore, seven candidate biomarkers (RYR1, KNG1, GSN, FETB, B2M, SHBG, and PTK2B) displayed AUC values above to 95.1% in

differentiating OP from OS (FDR *p*-value < 0.05) (Supplementary Fig. 4 G–I).

Additionally, three combined models were generated using six proteins with individual AUC > 90% for OP vs. N, seven with AUC > 70% for OS vs. N, and seven with AUC > 90% for OP vs. OS. As shown in Fig. 5, the individual ROC of candidate biomarkers increased the AUC when they were combined (red), particularly between OS vs. N.

Table 2 Candidate biomarker proteins related to BMD

| UniProtKB | Protein name | Peptide count | Unique peptides | Mean N | Mean OS | Mean OP | OS vs. N log ₂ FC | OP vs. N log ₂ FC | OP vs. OS log ₂ FC | Untargeted quantitative proteomic studies |
|-----------|---|---------------|-----------------|--------|---------|---------|------------------------------|------------------------------|-------------------------------|---|
| P21817 | Ryanodine receptor 1 (RYR1) | 45 | 4 | 36.6 | 64.5 | 5606 | 0.85** | 7.26** | 6.64** | |
| P48740 | Mannan-binding lectin serine protease 1 (MASP1) | 27 | 2 | 16.7 | 16 | 453 | -0.15 | 4.76* | 4.82* | [16, 29] |
| P04278 | Sex hormone-binding globulin (SHBG) | 14 | 6 | 628 | 852 | 1836 | 0.48 | 1.53** | 1.11** | [30] |
| Q14289 | Protein-tyrosine kinase 2-beta (PTK2B) | 9 | 2 | 1239 | 1711 | 2923 | 0.48 | 1.26** | 0.77** | |
| P01042-2 | Isoform LMW of Kininogen-1 (KNG1) | 39 | 6 | 8895 | 8443 | 22,485 | -0.15 | 1.32** | 1.41** | [19] |
| P02647 | Apolipoprotein A-I (APOA1) | 81 | 37 | 5399 | 7229 | 11,474 | 0.38 | 1.07** | 0.66* | [16, 29] |
| P06396 | Gelsolin (GSN) | 117 | 57 | 12,998 | 12,208 | 27,799 | -0.15 | 1.07** | 1.07** | [16, 19, 29] |
| Q9UGM5 | Fetuin-B (FETB) | 22 | 11 | 725 | 644 | 1468 | -0.15 | 1.07** | 1.19** | [16] |
| P61769 | Beta-2-microglobulin (B2M) | 9 | 6 | 218 | 241 | 699 | 0.14 | 1.68** | 1.53** | [29, 30] |
| P02652 | Apolipoprotein A-II (APOA2) | 35 | 16 | 13,848 | 9497 | 8755 | -0.51** | -0.74** | -0.11** | [16] |
| P02042 | Hemoglobin subunit delta (HBD) | 30 | 12 | 1544 | 432 | 230 | -1.73 | -2.32** | -0.43 | [28, 29] |
| Q15413 | Ryanodine receptor 3 (RYR3) | 55 | 7 | 244 | 158 | 75.8 | -0.74 | -1.74** | -1.05** | |

N normal, OS osteopenia, OP osteoporosis

*FDR-corrected p -value < 0.05, t -test

**FDR-corrected p -value < 0.01, t -test

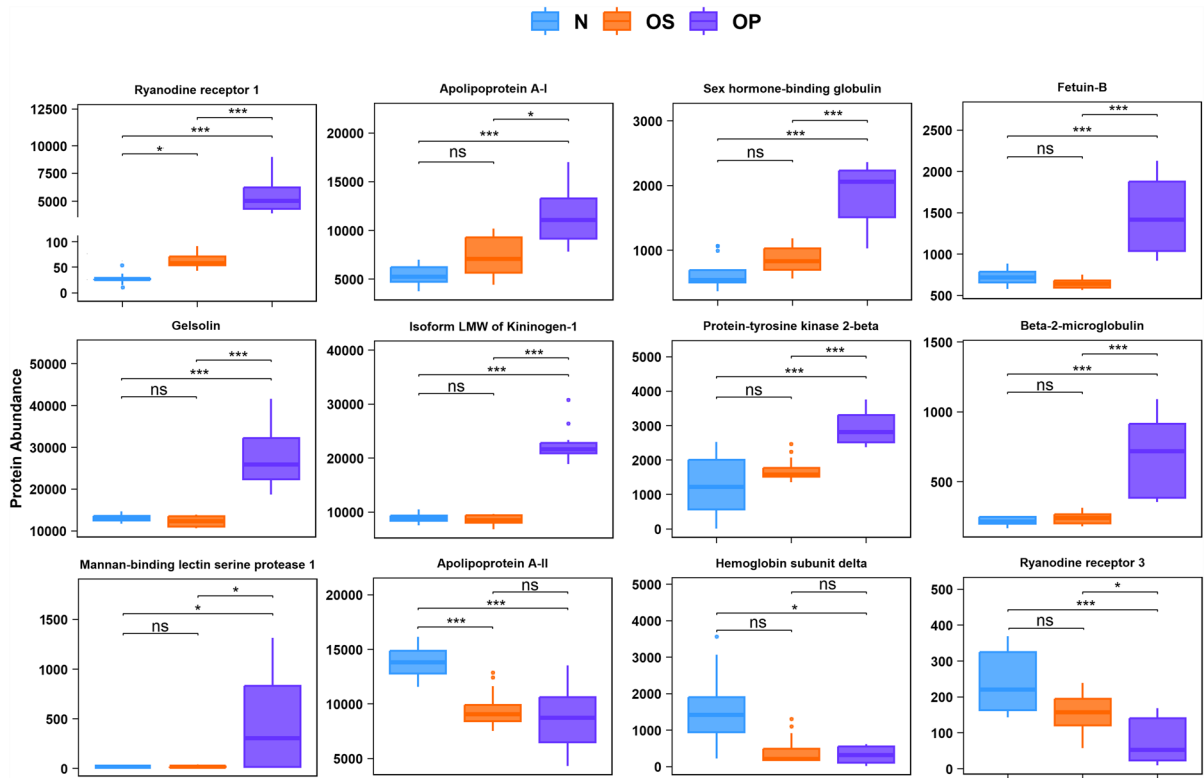


Fig. 4 Comparison of the serum levels of these 12 proteins between the three study groups. Box plot showing the plasma levels in N, OS, and OP groups of each differentially expressed

protein selected as a potential candidate. *FDR-corrected p -value < 0.05; **FDR-corrected p -value < 0.01; ***FDR-corrected p -value < 0.001. ns, not significant

Correlation analysis

The correlation analysis was performed to identify the relationship between the proteins selected as candidate biomarkers and clinical variables (Supplementary Table 6). The hip T-score, femoral neck, and hip BMD values were negatively correlated with SHBG, KNG1, RYR1, APOA1, B2M, GSN, and FETB serum levels (FDR p -value < 0.05). Meanwhile, APOA2, HBD, and RYR3 serum levels were positively correlated with hip T-score, femoral neck, and hip BMD (FDR p -value < 0.05) (Fig. 6).

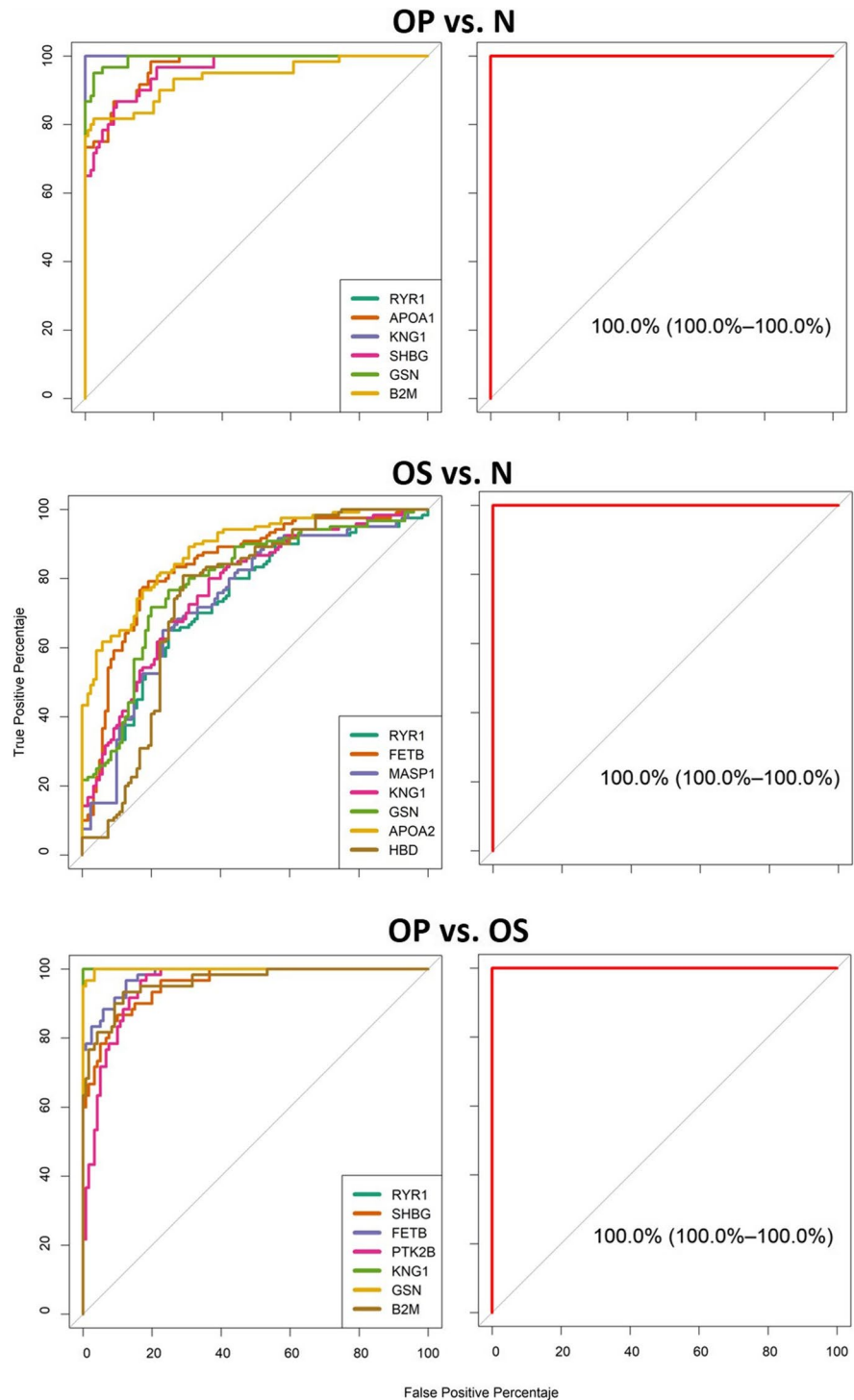
Discussion

Osteoporosis is a chronic progressive bone disease characterized by low bone mineral density and impaired bone microarchitecture. Herein, we conducted a serum proteomic analysis to investigate

differentially expressed proteins between postmenopausal women with normal and low BMD. Our study revealed a distinctive profile between normal (N), osteopenic (OS), and osteoporotic (OP) women. When the OP group was compared to the N group, we observed 214 DEPs; from them, 128 were upregulated and 86 downregulated. From the comparison between the OS and N groups, 14 DEPs were identified, seven upregulated and seven downregulated. To establish a possible role for DEPs, functional analysis was performed by gene ontology (GO) enrichment. Interestingly, most DEPs were associated with microtubules, cilium or flagellum-dependent cell motility, immune response, and complement activation.

Previous studies have analyzed the quantitative proteome profile from osteopenic and osteoporotic subjects in different populations [16, 19, 28–31]. Recently, Al-Ansari et al. analyzed the proteomic profiles of Saudi postmenopausal women and men, finding only 68 DEPs significantly associated with

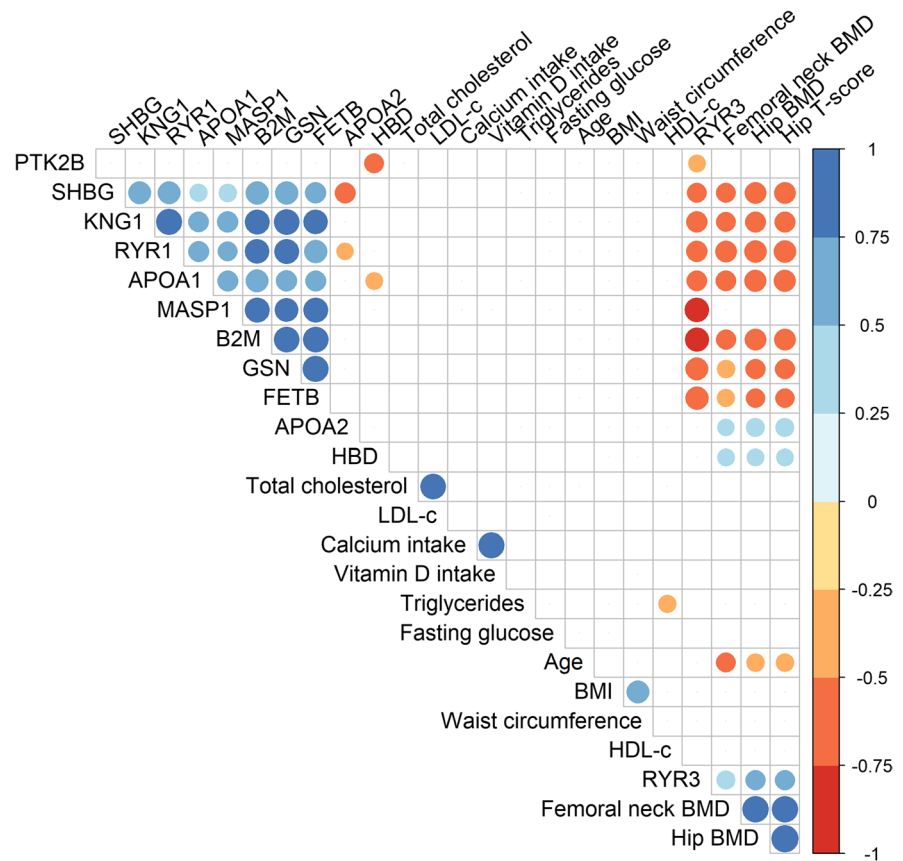
Fig. 5 Receiver operating characteristic (ROC) curves for each candidate biomarker and combined models. The first plot was performed with candidate biomarkers selected, and the second plot was generated by combining candidate biomarkers (in red). Candidate biomarkers selected between OP vs. N had individual AUC > 90%, OS vs. N AUC > 70%, and OP vs. OS AUC > 90%. All ROC curves were generated using the protein abundance adjusted for age. AUC and 95% CI of individual candidate biomarker are shown in Supplementary Fig. 3



low BMD [28]. Although the OS and OP groups were recruited from the same Hospital, several factors might have affected the differential expression

findings, for example, technical replicates were not included, and the number of confounding factors in the experimental design. Furthermore, Huang

Fig. 6 Correlation matrix of clinical data versus candidate biomarker proteins. Blue indicates a positive correlation and red indicates a negative correlation with an FDR p -value < 0.05. The circles shown have a r -value > 0.45 or < -0.45. Color intensity and the size of the circle are proportional to the Spearman correlation coefficients



et al. reported the plasma proteomic profile from postmenopausal women with and without OP. The differential abundance analysis showed that the proteome of individuals with OP was significantly different from the N group. In contrast, the proteome of the OS group was more similar to the N group [16]. The present study observed similar findings, where the proteomic profiles obtained from the OS and N groups had considerable overlap. Nevertheless, our results are supported by the experimental design, where four pooled samples with three replicates were analyzed to avoid random variation. Prior research focused on identifying circulating protein markers has studied serum microvesicles. Hou et al. reported more than one hundred DEPs in OS and OP individuals, from which 19 were upregulated in both low BMD groups compared to the N group [29]. Although some potential protein markers were identified, the number of processed samples per group was small. Another study analyzing plasma exosomes from Chinese men and postmenopausal

women revealed 45 DEPs, four were indicative of OP [31]. Another serum proteomics study in non-Hispanic white men ≥ 65 years old showed 339 DEPs associated with accelerated BMD loss [30]. Although the study controlled the technical variation of the proteomic measures, the differentially abundant proteins resulted from comparing groups categorized based on the longitudinal change of BMD in a cohort of community-dwelling older men [30, 32]. Previously, our group reported a differential serum proteome profile from postmenopausal women with low BMD compared to postmenopausal women with normal BMD. However, due to the technical limitation of two-dimensional differential gel electrophoresis (2D-DIGE), only 27 spots were identified when comparing low BMD versus normal [19]. These findings indicate that the experimental design, specifically the confounding factors (age, sex, and medication), might have affected the differential abundance of proteins, which may provide prognostic information or serve as biomarkers.

Based on the role on bone metabolism, we selected 12 DEPs as candidate biomarkers, one (RYR1) was found upregulated in the OS and OP groups, eight (APOA1, SHBG, FETB, MASP1, PTK2B, KNG1, GSN, and B2M) were upregulated only in the OP group. At the same time, three proteins (APOA2, RYR3, and HBD) were downregulated in OS or OP groups. Among these proteins, RYR1, RYR3, and GSN are related to bone metabolism, particularly in osteoclast differentiation and calcium. According to the literature, ryanodine receptors (RYRs) are a family of intracellular ion channels that comprise isoforms with three subtypes: RYR1, RYR2, and RYR3. RYR1 is expressed in skeletal muscle, lymphocytes, and osteoblastic cells [33]. RYR2 is the predominant isoform expressed in cardiac muscle, neurons, visceral, and arterial smooth muscle. RYR3 is the least studied of the RYR isoforms, RYR3 is expressed in epithelial cells, the brain, and smooth muscle. A previous study demonstrated the role of RYR3 on bone fractures in birds [34], suggesting that RYR3 may transmit Ca^{2+} signaling through the Ca^{2+} release pathway. To the best of our knowledge, proteomic data regarding serum levels of the RYRs have not been reported in studies focused on osteoporosis. However, it is well known that bone turnover is regulated by the RYRs, together with inositol-1,4,5-trisphosphate receptors (IP3Rs) and the calcium release-activated calcium channels (CRACs) in osteoclast [35]. Moreover, in Chinese patients with sporadic Paget's disease of bone (PDB), mutations in *RYR1* and *RYR3* have been identified [36]. A case report article described a 57-year-old woman with congenital neuromuscular myopathy and early osteoporosis carrying an *RYR1* heterozygous mutation [37]. These results suggest that *RYR1* and *RYR3* genes play essential roles in BMD control and could be involved in the physiopathology of osteoporosis. Additional studies are needed to validate whether serum RYR1 and RYR3 levels may be potential biomarkers of low BMD (osteopenia and osteoporosis).

Gelsolin (GSN) is one of the most abundant and potent actin filaments severing, capping, and nucleating proteins, which calcium and pH regulate processing and assembly. This process is critical for podosome assembly, where a rapid polymerization/depolymerization of actin occurs [38]. A model of gelsolin-deficient mice showed that osteoclasts presented abnormal actin cytoskeletal architecture and

reduced rates of osteoclast motility, contributing to reduced bone resorption in vivo and blocking the podosome-associated signal transduction [39]. In our study, GSN was upregulated only in the OP group and negatively correlated with BMD. These data are consistent with a previous proteomic analysis in plasma, where GSN levels were negatively correlated with total hip BMD in Chinese postmenopausal women [40]. GSN is a protein involved in actin cytoskeletal organization [41]. Previous studies have shown that it plays an essential role in osteoclasts. GSN deficiency reduces bone resorption and increases bone mass and strength in mice [39]. Furthermore, GSN serves as a regulator of androgen-mediated effects on osteoclastogenesis and bone resorption [42]. Taken together, these studies reinforce the importance of GSN for bone metabolism, and its potential as a biomarker involved in the molecular pathogenesis of OP. However, further studies are needed to determine the effect of plasma GSN on bone resorption and formation.

The specific effects of Fetuins on OS and OP are still unclear. Previous studies have reported that Fetuin-A (FETA) is associated with bone formation and remodeling [43, 44]. FETA inhibits mineralization by blocking basic calcium phosphate precipitation and regulating apatite formation during this process [45]. In mice with Heterotopic Ossification (HO), the recombinant FETA inhibited the hyperinflammation and prevented HO and associated bone mass loss, suggesting that FETA is a potential therapeutic option for treating HO [46]. In our proteomic analysis, Fetuin-B (FETB) was overexpressed in the OP group, and its abundance negatively correlated with BMD. Likewise, a previous report showed higher serum levels of FETB in osteoporotic women than in controls. Also, FETB correlated positively with femoral and lumbar BMD [47]. Although the evidence regarding the role of FETB on bone metabolism is scarce, some studies suggest a similar physiologic effect as the one described for FETA [48]. Therefore, FETB might be involved in the pathophysiology of osteoporosis [49]. Taking together previous reports and the results of our study, FETB might be a potential biomarker for the early detection of bone mass loss in postmenopausal women.

Several studies have reported that dyslipidemia could affect bone homeostasis, leading to loss of bone mass. Particularly apolipoproteins, apolipoprotein A1 (APOA1) is the most common form in plasma

and extravascular compartments, followed by apolipoprotein A2 (APOA2). In our study, APOA1 was upregulated, and APOA2 was downregulated in the OP group. Pliatsika et al. found that APOA1 serum levels were negatively associated with lumbar T-score in postmenopausal Greek women (<53 years old) [50]. A cross-sectional study from the Third National Health and Nutrition Examination Survey (NHANES III), where most enrolled participants were Non-Hispanic White, demonstrated that participants with osteoporosis had higher levels of APOA1 than those without osteoporosis [51]. In contrast, the succinyl-proteome profiling of postmenopausal Chinese women revealed that APOA1 was downregulated and APO2 was upregulated in the OP group [52]. These findings suggest that APO1 and APO2 play a vital role in maintaining bone density. However, it should be noted that the Mexican population has a strong genetic factor that could influence plasma lipid levels [53–55]. Additional studies attempting to associate APO1 and APO2 with BMD would help establish the true significance of these apolipoproteins in bone homeostasis.

Emerging evidence has suggested that the immune and skeletal systems are closely related. Our study found three proteins related to the immune system, upregulated in the OP group, the mannan-binding lectin serine protease 1 (MASP1), isoform LMW of Kininogen-1 (KNG1), and beta 2-microglobulin (B2M). MASP1 initiates the lectin pathway of the complement cascade. It activates MASP2, C2, or C3, triggering the formation of a pore complex on the membrane of target cells, causing cell lysis [56]. In addition, studies in murine models have demonstrated that the C3 or C5 signaling pathway regulates osteoclast differentiation, whereas blocking C3 in bone marrow cells in culture attenuates osteoclast maturation [57–59]. These data demonstrate that the complement pathway could be a possible mechanism involved in bone remodeling. Nevertheless, additional studies are necessary to determine the contribution of MASP-1 and the complement pathway in osteoporosis.

KNG1, a precursor protein of vasoactive Kinin, participates in inflammation and innate immunity. Consistently with our previous study [19], KNG1 was upregulated in the OS group. KNG1 has also been associated with Paget's disease and modulates bone marrow-derived stromal/preosteoblast cell

proliferation and suppresses etoposide-induced apoptosis through ERK and HSP27 activation, respectively [60]. Based on these findings, we speculate that KNG1 is highly associated with bone metabolism in osteoporosis.

Beta 2-microglobulin (B2M) is a component of class I of the major histocompatibility complex (MHC), and it is known as a marker of aging and cellular senescence [61]. The present study observed a higher abundance of B2M in the osteoporotic group. Similar results have been reported by Huo et al. and Nielson et al. [29, 30]. Ripoll et al. reported that B2M increased after calcitonin treatment, revealing a potential role as a biological marker related to bone remodeling [62]. In addition, B2M has a role in NF- κ B signaling because it activates the production of pro-inflammatory and inflammatory cytokines and proteins that degrade bone [63]. B2M induces a time and dose-dependent calcium release and a significant release and expression of IL-6 from osteoblasts, activating bone resorption [64]. Our results and previous reports on the action of B2M on bone resorption suggest that therapies focused on increasing B2M expression could help prevent BMD loss.

Several remaining proteins reported here have a known relationship with bone development or metabolism. For example, the sex hormone-binding globulin (SHBG) is a plasma glycoprotein that binds with high affinity to sex steroids, regulating their bioavailability and access into target cells. SHBG has been implicated in several diseases, including osteoporosis. A systematic review of serum SHBG, including 16 studies, reported that higher levels of SHBG predicted an increased risk of fracture in older adults [65]. Besides, a large cross-sectional study in adults from the USA demonstrated that serum SHBG could be considered an independent predictor of BMD [66]. Our data showed increased serum levels of SHBG in the OS and OP groups. Also, SHBG levels correlated negatively with BMD and positively with HDL-c. Further studies should aim to elucidate if SHBG may play a role in bone homeostasis and could be further evaluated as a serum biomarker for osteoporosis.

Furthermore, the potential diagnosis of these protein biomarker candidates was evaluated by ROC analysis. RYR1, KNG1, and GSN, which showed individually the highest diagnostic capacity for osteoporosis (AUC > 99%), were negatively correlated with postmenopausal bone loss. For osteopenia, FETB,

GSN, and KNG1 negatively correlated with BMD, with $AUC > 70\%$. Remarkably, the combination of biomarkers with the highest AUC value between groups increased ($AUC = 100\%$) compared to each individual candidate. Therefore, the distinctive signature of these biomarkers could significantly improve diagnostic performance. It revealed the potential as a diagnostic tool for populations by detecting serum proteins.

Our study has several limitations that need to be considered. First, interindividual variation, the proteomic analysis was performed with pooled samples and three replicates per pool. Extreme sampling adopted in our study is an economic strategy and has been validated in other proteomic studies. It is a more representative and powerful approach for detecting potential biomarkers in small sample sizes [14, 16, 40, 67, 68]. At the same time, potential biomarkers were selected only if they were present in all groups to avoid bias due to detection. Furthermore, our study included a review of proteomic data from available clinical studies. The most important limitation of the present work is the need for validation of the selected proteins and follow-up of the patients. However, a larger cohort is needed to validate the diagnosis sensibility and specificity of the selected potential biomarkers. We plan to conduct future studies incrementing the number of patients with osteoporosis and a group with fragility fractures. Second, different combinations of biomarkers should be tested to evaluate the predictive potential for the disease. Together, biochemical markers of bone turnover and resorption and known clinical risk factors could improve sensitivity and specificity. Despite these limitations, this novel study formulates several hypotheses about the proteins involved in the pathogenesis of low BMD in Mexican population. Finally, these findings suggest that common pathways may exist in the pathogenesis of metabolic-related diseases, such as lipid metabolism, osteoporosis, and cardiovascular diseases. This proteomics analysis provides essential insights for future research for identification of the affected individuals at the early stages of the disease.

Conclusions

This study used a label-free proteomics approach to analyze the serum proteomic profile of postmenopausal women with low BMD (OS and OP) at the hip compared

to women with normal BMD. Our results revealed significant changes in the serum proteome in osteopenic and osteoporotic individuals compared to normal women. Literature-based screening identified a distinctive panel of 12 DEPs as potential biomarkers for detecting low BMD. In addition, our study identified three novel proteins potentially involved in bone metabolism: RYR1, FETB, and MASP1, opening the possibility of being associated with OP. The results of this study provide information on some of the pathways and proteins involved in bone metabolism. This knowledge could be the platform for new research focused on bone disease and its medical management. However, additional validation is needed to determine the role of each protein and its association with low BMD.

Acknowledgements The authors thankfully acknowledge the technical support provided by Sergio A Román-González PhD and Monserrat Rojano-Vilchis, for the depletion of the most abundant proteins, performed in the Proteomics Core Unit at the INMEGEN, Mexico City, Mexico. Quantitative mass spectrometry-based proteomics was performed in Genomics, Proteomics and Metabolomics Core Facility (UGPM), LaNSE, CINVESTAV-IPN. We want to thank to ChemE. Nataly Ramos Buendía for their support during sample preparation and LC-MS analysis. The authors also wish to thank the staff of the Epidemiological Research Unit and Services of Health-IMSS, Cuernavaca, Morelos.

Author contribution D.I.A.-B., A.B.-C., A.H.-B., and R.V.-C. contributed to conception and design of the study. J.S. and B.R.-P. collected and reviewed the data of the study. E.R. performed the label-free quantitative proteomics and provided raw proteomic data. J.P.R.-G. provision of study materials. D.I.A.-B., A.B.-C., I.A., E.R., and B.R.-P. performed the bioinformatic and statistical analysis. D.I.A.-B., A.B.-C., A.H.-B., and R.V.-C. drafted and revised the manuscript. All the authors have reviewed the manuscript and approved the submitted version.

Funding This work was funded by the Consejo Nacional de Ciencia y Tecnología (Grant Ciencia de Frontera CF2019 – 102962), and received partial funding from Instituto Nacional de Medicina Genómica (314–07/2017/I and 266–17/2016/I). A.B.-C. is supported by a Postdoctoral Fellowship from the Consejo Nacional de Humanidades, Ciencia y Tecnología (CONAHCYT-Estancia Posdoctoral de Incidencia Inicial 2022 with CVU 508876).

Data Availability The authors confirm that the data supporting the findings of this study are available within the article and its supplementary materials.

Declarations

Conflict of interest The authors declare no competing interests.

References

- Reginster JY, Burlet N. Osteoporosis: a still increasing prevalence. *Bone*. 2006;38(2 Suppl 1):4–9. <https://doi.org/10.1016/J.BONE.2005.11.024>.
- Gossiel F, Altaher H, Reid DM, et al. Bone turnover markers after the menopause: T-score approach. *Bone*. 2018;111:44–8. <https://doi.org/10.1016/J.BONE.2018.03.016>.
- Johnell O, Kanis JA. An estimate of the worldwide prevalence and disability associated with osteoporotic fractures. *Osteoporos Int*. 2006;17(12):1726–33. <https://doi.org/10.1007/S00198-006-0172-4>.
- Becker DJ, Kilgore ML, Morrisey MA. The societal burden of osteoporosis. *Curr Rheumatol Rep*. 2010;12(3):186–91. <https://doi.org/10.1007/S11926-010-0097-Y>.
- Carlos F, Clark P, Galindo-Suárez RM, Chico-Barba LG. Health care costs of osteopenia, osteoporosis, and fragility fractures in Mexico. *Arch Osteoporos*. 2013;8(1):125. <https://doi.org/10.1007/S11657-013-0125-4>.
- Aziziyeh R, Amin M, Habib M, et al. A score-card for osteoporosis in four Latin American countries: Brazil, Mexico, Colombia, and Argentina. *Arch Osteoporos*. 2019;14(1):69. <https://doi.org/10.1007/S11657-019-0622-1>.
- Albergaria BH, Chalem M, Clark P, Messina OD, Pereira RMR, Vidal LF. Consensus statement: osteoporosis prevention and treatment in Latin America—current structure and future directions. *Arch Osteoporos*. 2018;13(1):90. <https://doi.org/10.1007/S11657-018-0505-X>.
- Choksi P, Jepsen KJ, Clines GA. The challenges of diagnosing osteoporosis and the limitations of currently available tools. *Clin Diabetes Endocrinol*. 2018;4(1):12. <https://doi.org/10.1186/S40842-018-0062-7>.
- Zhang AH, Sun H, Yan GL, Han Y, Wang XJ. Serum proteomics in biomedical research: a systematic review. *Appl Biochem Biotechnol*. 2013;170(4):774–86. <https://doi.org/10.1007/S12010-013-0238-7>.
- Migliorini F, Maffulli N, Spiezia F, Tingart M, Maria PG, Riccardo G. Biomarkers as therapy monitoring for postmenopausal osteoporosis: a systematic review. *J Orthop Surg Res*. 2021;16(1):318. <https://doi.org/10.1186/S13018-021-02474-7>.
- Szulc P, Delmas PD. Biochemical markers of bone turnover: potential use in the investigation and management of postmenopausal osteoporosis. *Osteoporos Int*. 2008;19(12):1683–704. <https://doi.org/10.1007/S00198-008-0660-9>.
- Deutsch EW, Omenn GS, Sun Z, et al. Advances and utility of the human plasma proteome. *J Proteome Res*. 2021;20(12):5241–63. <https://doi.org/10.1021/ACS.JPROTEOME.1C00657>.
- Greco V, Piras C, Pieroni L, Urbani A. Direct assessment of plasma/serum sample quality for proteomics biomarker investigation. *Methods Mol Biol*. 2017;1619:3–21. https://doi.org/10.1007/978-1-4939-7057-5_1.
- Deng FY, Liu YZ, Li LM, et al. Proteomic analysis of circulating monocytes in Chinese premenopausal females with extremely discordant bone mineral density. *Proteomics*. 2008;8(20):4259–72. <https://doi.org/10.1002/PMIC.200700480>.
- Lv M, Cui C, Chen P, Li Z. Identification of osteoporosis markers through bioinformatic functional analysis of serum proteome. *Medicine*. 2020;99(39):e22172. <https://doi.org/10.1097/MD.00000000000022172>.
- Huang D, Wang Y, Lv J, et al. Proteomic profiling analysis of postmenopausal osteoporosis and osteopenia identifies potential proteins associated with low bone mineral density. *PeerJ*. 2020;8:e9009. <https://doi.org/10.7717/PEERJ.9009/SUPP-8>.
- Zhang LI, Li CW, Liu K, et al. Discovery and identification of serum succinyl-proteome for postmenopausal women with osteoporosis and osteopenia. *Orthop Surg*. 2019;11(5):784–93. <https://doi.org/10.1111/OS.12519>.
- Hlaing TT, Compston JE. Biochemical markers of bone turnover - uses and limitations. *Ann Clin Biochem*. 2014;51(Pt 2):189–202. <https://doi.org/10.1177/0004563213515190>.
- Martínez-Aguilar MM, Aparicio-Bautista DI, Ramírez-Salazar EG, et al. Serum proteomic analysis reveals vitamin D-binding protein (VDBP) as a potential biomarker for low bone mineral density in Mexican postmenopausal women. *Nutrients*. 2019;11(12):2853. <https://doi.org/10.3390/NU11122853>.
- Denova-Gutiérrez E, Flores YN, Gallegos-Carrillo K, et al. Health workers cohort study: methods and study design. *Salud Publica Mex*. 2016;58(6):708–16. <https://doi.org/10.21149/SPM.V58I6.8299>.
- Kanis JA, Glüer CC. An update on the diagnosis and assessment of osteoporosis with densitometry. Committee of Scientific Advisors, International Osteoporosis Foundation. *Osteoporos Int*. 2000;11(3):192–202. <https://doi.org/10.1007/S001980050281>.
- Kanis JA, Kanis JA. Assessment of fracture risk and its application to screening for postmenopausal osteoporosis: synopsis of a WHO report. WHO Study Group. *Osteoporos Int*. 1994;4(6):368–81. <https://doi.org/10.1007/BF01622200>.
- Ortega-Lozano AJ, Jiménez-Urbe AP, Aranda-Rivera AK, et al. Expression profiles of kidney mitochondrial proteome during the progression of the unilateral ureteral obstruction: focus on energy metabolism adaptations. *Metabolites*. 2022;12(10):936. <https://doi.org/10.3390/METABO12100936>.
- Rios-Castro E, Souza GHMF, Delgadillo-Alvarez DM, et al. Quantitative proteomic analysis of MARC-145 cells infected with a Mexican porcine reproductive and respiratory syndrome virus strain using a label-free based DIA approach. *J Am Soc Mass Spectrom*. 2020;31(6):1302–12. <https://doi.org/10.1021/JASMS.0C00134>.
- Li GZ, Vissers JPC, Silva JC, Golick D, Gorenstein MV, Geromanos SJ. Database searching and accounting of multiplexed precursor and product ion spectra from the data independent analysis of simple and complex peptide mixtures. *Proteomics*. 2009;9(6):1696–719. <https://doi.org/10.1002/PMIC.200800564>.
- Käll L, Storey JD, MacCoss MJ, Noble WS. Assigning significance to peptides identified by tandem mass spectrometry using decoy databases. *J Proteome Res*. 2008;7(1):29–34. <https://doi.org/10.1021/PR700600N>.

27. Yu G, Wang LG, Han Y, He QY. clusterProfiler: an R package for comparing biological themes among gene clusters. *OMICS*. 2012;16(5):284–7. <https://doi.org/10.1089/OMI.2011.0118>.
28. Al-Ansari MM, Aleidi SM, Masood A, et al. Proteomics profiling of osteoporosis and osteopenia patients and associated network analysis. *Int J Mol Sci*. 2022;23(17):10200. <https://doi.org/10.3390/IJMS231710200>.
29. Huo C, Li Y, Qiao Z, et al. Comparative proteomics analysis of microvesicles in human serum for the evaluation of osteoporosis. *Electrophoresis*. 2019;40(14):1839–47. <https://doi.org/10.1002/ELPS.201900130>.
30. Nielson CM, Wiedrick J, Shen J, et al. Identification of hip BMD loss and fracture risk markers through population-based serum proteomics. *J Bone Miner Res*. 2017;32(7):1559–67. <https://doi.org/10.1002/JBMR.3125>.
31. Chen M, Li Y, Lv H, Yin P, Zhang L, Tang P. Quantitative proteomics and reverse engineer analysis identified plasma exosome derived protein markers related to osteoporosis. *J Proteomics*. 2020;228:103940. <https://doi.org/10.1016/J.JPROT.2020.103940>.
32. Cawthon PM, Ewing SK, McCulloch CE, et al. Loss of hip BMD in older men: the osteoporotic fractures in men (MrOS) study. *J Bone Miner Res*. 2009;24(10):1728. <https://doi.org/10.1359/JBMR.090419>.
33. Adebajo OA, Biswas G, Moonga BS, et al. Novel biochemical and functional insights into nuclear Ca(2+) transport through IP(3)Rs and RyRs in osteoblasts. *Am J Physiol Renal Physiol*. 2000;278(5):F784–91. <https://doi.org/10.1152/AJPRENAL.2000.278.5.F784>.
34. Wei H, Bi Y, Wang Y, et al. Serum bone remodeling parameters and transcriptome profiling reveal abnormal bone metabolism associated with keel bone fractures in laying hens. *Poult Sci*. 2023;102(4):102438. <https://doi.org/10.1016/J.PSJ.2022.102438>.
35. Robinson LJ, Blair HC, Barnett JB, Zaidi M, Huang CLH. Regulation of bone turnover by calcium-regulated calcium channels. *Ann N Y Acad Sci*. 2010;1192:351–7. <https://doi.org/10.1111/J.1749-6632.2009.05219.X>.
36. Tao X, Liu L, Yang X, et al. Clinical characteristics and pathogenic gene identification in Chinese patients with Paget's disease of bone. *Front Endocrinol (Lausanne)*. 2022;13:850462. <https://doi.org/10.3389/FENDO.2022.850462>.
37. Tariq E, Mirza L. Early osteoporosis in RYR1-related central core disease. *J Endocr Soc*. 2021;5(Suppl 1):A191. <https://doi.org/10.1210/JENDSO/BVAB048.387>.
38. Chen ZH, Wu JJ, Guo DY, et al. Physiological functions of podosomes: from structure and function to therapy implications in osteoclast biology of bone resorption. *Ageing Res Rev*. 2023;85:101842. <https://doi.org/10.1016/J.ARR.2023.101842>.
39. Chellaiah M, Kizer N, Silva M, Alvarez U, Kwiatkowski D, Hruska KA. Gelsolin deficiency blocks podosome assembly and produces increased bone mass and strength. *J Cell Biol*. 2000;148(4):665–78. <https://doi.org/10.1083/JCB.148.4.665>.
40. Wang WY, Ge B, Shi J, et al. Plasma gelsolin is associated with hip BMD in Chinese postmenopausal women. *PLoS One*. 2018;13(5):e0197732. <https://doi.org/10.1371/JOURNAL.PONE.0197732>.
41. Silacci P, Mazzolai L, Gauci C, Stergiopoulos N, Yin HL, Hayoz D. Gelsolin superfamily proteins: key regulators of cellular functions. *Cell Mol Life Sci*. 2004;61(19–20):2614–23. <https://doi.org/10.1007/S00018-004-4225-6>.
42. Saltel F, Chabadel A, Bonnelye E, Jurdic P. Actin cytoskeletal organisation in osteoclasts: a model to decipher transmigration and matrix degradation. *Eur J Cell Biol*. 2008;87(8–9):459–68. <https://doi.org/10.1016/J.EJCB.2008.01.001>.
43. Toroian D, Price PA. The essential role of fetuin in the serum-induced calcification of collagen. *Calcif Tissue Int*. 2008;82(2):116–26. <https://doi.org/10.1007/S00223-007-9085-2>.
44. Özkan E, Özkan H, Bilgiç S, et al. Serum fetuin-A levels in postmenopausal women with osteoporosis. *Turk J Med Sci*. 2014;44(6):985–8. <https://doi.org/10.3906/SAG-1308-28>.
45. Schäfer C, Heiss A, Schwarz A, et al. The serum protein alpha 2-Heremans-Schmid glycoprotein/fetuin-A is a systemically acting inhibitor of ectopic calcification. *J Clin Invest*. 2003;112(3):357–66. <https://doi.org/10.1172/JCI17202>.
46. Kan C, Yang J, Fan H, et al. Fetuin-A is an immunomodulator and a potential therapeutic option in BMP4-dependent heterotopic ossification and associated bone mass loss. *Bone Res*. 2022;10(1):62. <https://doi.org/10.1038/S41413-022-00232-X>.
47. Xu ZH, He J, Zhang X, et al. Serum level of fetuin B is associated with osteoporosis: a 4-year prospective study in China. *Clin Invest Med*. 2018;41(1):E25–30. <https://doi.org/10.25011/CIM.V41I1.29460>.
48. Li L, Spranger L, Stobäus N, et al. Fetuin-B, a potential link of liver-adipose tissue cross talk during diet-induced weight loss-weight maintenance. *Nutr Diabetes*. 2021;11(1):31. <https://doi.org/10.1038/S41387-021-00174-Z>.
49. Jahnen-Dechent W, Heiss A, Schäfer C, Ketteler M. Fetuin-A regulation of calcified matrix metabolism. *Circ Res*. 2011;108(12):1494–509. <https://doi.org/10.1161/CIRCRESAHA.110.234260>.
50. Pliatsika P, Antoniou A, Alexandrou A, et al. Serum lipid levels and bone mineral density in Greek postmenopausal women. *Gynecol Endocrinol*. 2012;28(8):655–60. <https://doi.org/10.3109/09513590.2011.650766>.
51. Sun X, Wu X. Association of apolipoprotein A1 with osteoporosis: a cross-sectional study. *BMC Musculoskelet Disord*. 2023;24(1):157. <https://doi.org/10.1186/S12891-023-06264-6>.
52. Blair HC, Kalyvioti E, Papachristou NI, et al. Apolipoprotein A-1 regulates osteoblast and lipoblast precursor cells in mice. *Lab Invest*. 2016;96(7):763–72. <https://doi.org/10.1038/LABINVEST.2016.51>.
53. Valles V, Aguilar-Salinas CA, Gómez-Pérez FJ, et al. Apolipoprotein B and A-I distribution in Mexican urban adults: results of a nationwide survey. *Metabolism*. 2002;51(5):560–8. <https://doi.org/10.1053/meta.2002.31977>.
54. Aceves-Ramírez M, Valle Y, Casillas-Muñoz F, et al. Analysis of the APOB gene and apolipoprotein B serum levels in a Mexican population with acute coronary syndrome: association with the single nucleotide variants

- rs1469513, rs673548, rs676210, and rs1042034. *Genet Res (Camb)*. 2022;4901090. <https://doi.org/10.1155/2022/4901090>.
55. Gamboa R, Vargas-Alarcón G, Medina-Urrutia A, et al. Influence of the apolipoprotein E polymorphism on plasma lipoproteins in a Mexican population. *Hum Biol*. 2001;73(6):835–43. <https://doi.org/10.1353/HUB.2001.0080>.
 56. Verhamme IM, Leonard SE, Perkins RC. Proteases: pivot points in functional proteomics. *Methods Mol Biol*. 2019;1871:313. https://doi.org/10.1007/978-1-4939-8814-3_20.
 57. MacKay DL, Kean TJ, Bernardi KG, et al. Reduced bone loss in a murine model of postmenopausal osteoporosis lacking complement component 3. *J Orthop Res*. 2018;36(1):118–28. <https://doi.org/10.1002/JOR.23643>.
 58. Matsuoka K, Park KA, Ito M, Ikeda K, Takeshita S. Osteoclast-derived complement component 3a stimulates osteoblast differentiation. *J Bone Miner Res*. 2014;29(7):1522–30. <https://doi.org/10.1002/JBMR.2187>.
 59. Tu Z, Bu H, Dennis JE, Lin F. Efficient osteoclast differentiation requires local complement activation. *Blood*. 2010;116(22):4456–63. <https://doi.org/10.1182/BLOOD-2010-01-263590>.
 60. Tsuruga E, Rao DS, Baatz JE, Reddy SV. Elevated serum kininogen in patients with Paget's disease of bone: a role in marrow stromal/preosteoblast cell proliferation. *J Cell Biochem*. 2006;98(6):1681–8. <https://doi.org/10.1002/JCB.20874>.
 61. Althubiti M, Lezina L, Carrera S, et al. Characterization of novel markers of senescence and their prognostic potential in cancer. *Cell Death Dis*. 2014;5(11):e1528. <https://doi.org/10.1038/CDDIS.2014.489>.
 62. Ripoll E, Arribas I, Relea P, et al. Beta-2-microglobulin in diseases with high bone remodeling. *Calcif Tissue Int*. 1995;57(4):272–6. <https://doi.org/10.1007/BF00298882>.
 63. Boyce BF, Yao Z, Xing L. Functions of NF- κ B in Bone. *Ann N Y Acad Sci*. 2010;1192:367. <https://doi.org/10.1111/J.1749-6632.2009.05315.X>.
 64. Balint E, Marshall CF, Sprague SM. Role of interleukin-6 in beta2-microglobulin-induced bone mineral dissolution. *Kidney Int*. 2000;57(4):1599–607. <https://doi.org/10.1046/J.1523-1755.2000.00004.X>.
 65. Hidayat K, Du X, Shi BM. Sex hormone-binding globulin and risk of fracture in older adults: systematic review and meta-analysis of observational studies. *Osteoporos Int*. 2018;29(10):2171–80. <https://doi.org/10.1007/S00198-018-4600-Z>.
 66. Yang F, Yang D, Zhou Y, Wu J. Associations of sex hormone-binding globulin with bone mineral density among US adults, NHANES 2013–2016. *Int J Gen Med*. 2021;14:7707–17. <https://doi.org/10.2147/IJGM.S329992>.
 67. Guey LT, Kravic J, Melander O, et al. Power in the phenotypic extremes: a simulation study of power in discovery and replication of rare variants. *Genet Epidemiol*. 2011;35(4):236–46. <https://doi.org/10.1002/GEPI.20572>.
 68. Peloso GM, Rader DJ, Gabriel S, Kathiresan S, Daly MJ, Neale BM. Phenotypic extremes in rare variant study designs. *Eur J Hum Genet*. 2016;24(6):924. <https://doi.org/10.1038/EJHG.2015.197>.

Publisher's Note Springer Nature remains neutral with regard to jurisdictional claims in published maps and institutional affiliations.

Springer Nature or its licensor (e.g. a society or other partner) holds exclusive rights to this article under a publishing agreement with the author(s) or other rightsholder(s); author self-archiving of the accepted manuscript version of this article is solely governed by the terms of such publishing agreement and applicable law.